

A NEW MAXIMUM POWER POINT METHOD BASED ON A SLIDING MODE APPROACH & FUZZY LOGIC FOR SOLAR ENERGY HARVESTING

Thammineni Shravankumar¹, Adavipalli Chandana²

¹PG Scholar, Dept. Of EEE, SVCET, Srikakulam, Andhra Pradesh, (India)

²Assistant Professor, Dept. Of EEE, SVCET, Srikakulam, Andhra Pradesh, (India)

ABSTRACT

This paper presents a photovoltaic (PV) system with a maximum power point tracking (MPPT) facility. The goal of this work is to maximize power extraction from the photovoltaic generator (PVG). This goal is achieved using a sliding mode controller (SMC) that drives a boost converter connected between the PVG and the load. The system is modeled and tested under MATLAB/SIMULINK environment. In simulation, the sliding mode controller offers fast and accurate convergence to the maximum power operating point that outperforms the well-known perturbation and observation method (P&O). The sliding mode controller performance is evaluated during steady-state, against load varying and panel partial shadow (PS) disturbances. To confirm the above conclusion, a practical implementation of the maximum power point tracker based sliding mode controller on a hardware setup is performed on a dspace real time digital control platform. The data acquisition and the control system are conducted all around dspace 1104 controller board and its RTI environment. The experimental results demonstrate the validity of the proposed control scheme over a stand-alone real photovoltaic system.

1.INTRODUCTION

The rising of oil prices and increase in degree of pollution contrasted with the new provisions of sustainable development make alternative and renewable energy sources more attractive. Economic incentives and huge advancement in electronic technology promote the use of photovoltaic systems. The use of a converter on these photovoltaic systems is even more compelling as it increases their efficiency and reduces their costs. This work analyses the control of a stand-alone PV system. The success of a PV application depends on weather conditions where the power electronic devices help to increase the efficiency of the PV generator (PVG). Extracting maximum power from the PVG is a challenge. Maximum power point tracking (MPPT) controller accuracy is a key control in the device operation for successful PV applications. In general, a PV system is typically built around the following main components as shown in Fig.

(1) PVG that converts solar energy into electric energy.

- (2) DC–DC converter that manipulates produced DC voltage by the PVG to feed a load voltage demand.
- (3) Digital controller that drives the converter commutations accordingly to a MPPT capability.
- (4) Load

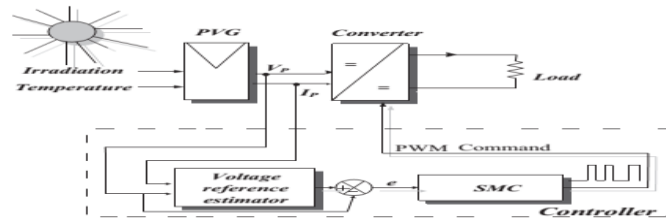


Fig.1 Synoptic diagram of PVG system.

In general, the MPPT control is challenging because the conditions that determine the amount of sun energy into the PVG may change at any time. As such, the PV system can be considered as non-linear complex. Numerous MPPT methods have been developed and implemented in previous studies including [1] perturb and observe (P&O) [2] incremental conductance (Inc-Cond) [3] fractional open-circuit voltage and short circuit current [4] fuzzy logic controller (FLC) approaches [5] and Adaptive neurofuzzy inference system, etc.. These algorithms consist of introducing a crisp value, positive or negative (decrease or increase), all around the actual PVG operating point. From the previous power point position, the trajectory of the new command value helps the algorithm to decide on the command output value. These techniques have high tracking accuracy under stable conditions. The main advantage of the SMC is its implementation simplicity, robustness, and great performance in different fields such as robotics and motor control. This paper proposes a new design of stable SMC for PV system control.

The proposed control methodology is built into two steps in order to control a PV system. The first step consists of an estimator synthesis of V_{ref} . This last corresponds to the (MPP) working voltage $V_{ref} = V_{MPP}$. The second is to perform the system tracking based on the developed SMC regulator for a boost converter and according to the estimated voltage value. The main objective in this work is to construct an MPP voltage-reference estimator that meets the MPP. The estimator is designed specifically in order to compute on-line the optimal voltage value V_{MPP} . In this paper, the proposed SMC uses the error between the measured voltage of the PV module and the voltage generated by the voltage reference estimator to adjust continuously the duty cycle (D) of the DC–DC Boost converter in order to eliminate this error. The reference voltage value is generated online with no need to know the actual irradiation. The paper is structured as follows: a brief description of the considered PV model; explanation of the entire proposed MPPT method; a detailed analysis of the voltage reference generator and a sliding mode controller method; partial shadowing (PS), Simulation results.

II. PHOTOVOLTAIC ENERGY CONVERSION

PV Generator Model:

One can substitute for a PV cell, an equivalent electric circuit that contains a power supply and a diode as shown in Fig. 2. Every PV generator is characterized by its maximum power point that is obtained in a defined voltage value, but due to the fact that this point is variable depending on the weather conditions; irradiation and temperature, creating a voltage reference estimator seems to be the best way in order to generate the right voltage value in any condition. The power source produces the I_{ph} current which depends on impinging irradiation. Through the diode flows current I_d . The current I_c feeding the load is the difference between I_{ph} and I_d which is reduced by the resistance R_s . This last represents resistances of the cell and connection among cells.

The node law gives:

$$I_c = I_{ph} - I_d - I_{sh} \tag{1}$$

The current I_{ph} can be evaluated as:

$$I_{ph} = \frac{G}{G_{ref}} (I_{rs_ref} + K_{SCT}(T_c - T_{c_ref})) \tag{2}$$

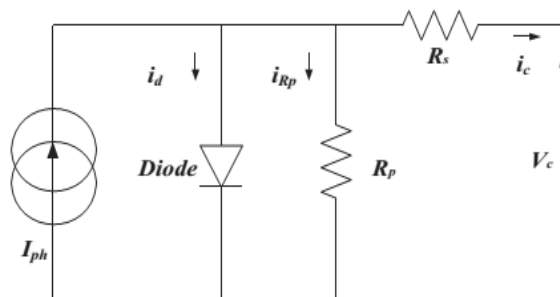


Fig. Simplified PV cell equivalent circuit

$$I_d = I_{rs} \left(\exp \frac{q(V_c + R_s I_c)}{\alpha k T} - 1 \right) \tag{3}$$

$$I_{sh} = \frac{1}{R_p} (V_c + R_s I_c) \tag{4}$$

The reverse saturation current at reference temperature can be approximately obtained as:

$$I_{rs} = \frac{I_{rs_ref}}{\exp \left[\frac{qV_{oc}}{n_s n \beta T_c} \right] - 1} \tag{5}$$

Finally, the cell current I_c can be given by:

$$I_c = I_{ph} - I_{rs} \left(\exp \frac{q(V_c + R_s I_c)}{\alpha k T} - 1 \right) - \frac{1}{R_p} (V_c + R_s I_c) \quad (6)$$

The modeling of a PVG as given in Fig. 3 depends on N_s and N_p that are the total numbers of series and parallel modules respectively

$$\begin{cases} I_p = N_p I_c \\ V_p = N_s n_s V_c \end{cases} \quad (7)$$

Finally the PVG current (I_p) can be given by,

$$I_p = N_p I_{ph} - N_p I_{rs} \left(\exp \frac{q}{\alpha k T} \left(\frac{V_p}{n_s N_s} + \frac{R_s I_p}{N_p} \right) - 1 \right) - \frac{N_p}{R_p} \left(\frac{V_p}{n_s N_s} + \frac{R_s I_p}{N_p} \right) \quad (8)$$

The terms containing R_s and R_p parameters could be eliminated by simplification assumption $R_p \& R_s$. Here the ideal model case is considered such as $R_s = 0$ and $R_p = 1$.

$$I_p = N_p I_{ph} - N_p I_{rs} \left(\exp \frac{q}{n \beta T_c} \left(\frac{V_p}{n_s N_s} \right) - 1 \right) \quad (9)$$

In this work, the ATERSA A55 PV manufactured module has been considered for simulation and practical validation purposes. This module has 36 series connected monocrystalline cells ($n_s = 36$). Modules ATERSA A55 (637 527 35) are characterized as being professional panels. They are built with mono-crystalline silicon cells that guarantee power production. The performance of solar cells is normally evaluated under the standard test condition, the irradiance is normalized to 1000 W/m², and the cell temperature is defined as 25 C.

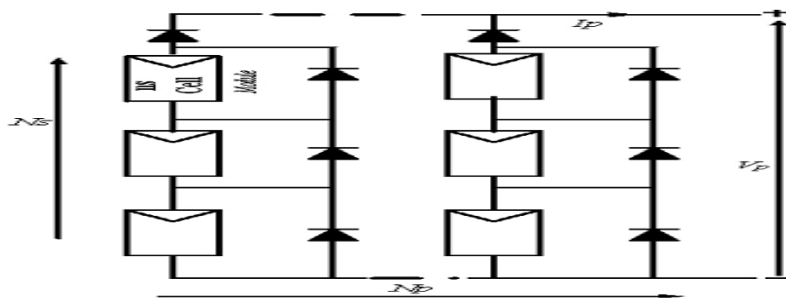


Fig. A PVG group of modules; N_s numbers in series and N_p in parallel.

In order to increase the power, four modules are connected in parallel to form the PV panel that will be used in this paper. The extreme I–V nonlinear characteristics are shown in Fig. These real characteristics are logged and plotted for different radiation values and an almost constant temperature.

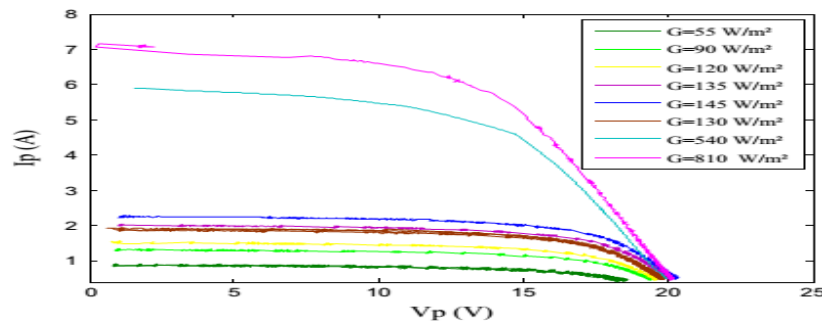


Fig. I–V characteristics for different irradiances

III. MPPT CONTROL

The Maximum Power Point Tracking (MPPT) control is a fundamental phase in order to obtain a good performance in a PVG system. Usually, the principle of this MPPT is based on adapting or varying the converter duty cycle (D) to finally bring the PVG working in its MPP. The Perturb & Observe is the most common method. However, it presents a lot of drawbacks. As a solution to overcome these drawbacks, a MPPT new control method which is based on SMC is proposed in this section.

3.1P&O Algorithm Principle:

Due to its simplicity, the P&O algorithm is the most popular. The principle of this controller is to provoke perturbation by acting on (decrease or increase) the PWM duty cycle command and observing the output PVG power reaction. If the present power $P(k)$ is greater than the previous computed one $P(k-1)$, then the perturbation direction is maintained. Otherwise, it is reversed. The P&O algorithm can be detailed as follows:

- When the ratio DP/DV is positive, the voltage must be increased, this yields

$$D(K) = D(K - 1) + \Delta D, (\Delta D : \text{crisp value})$$

- When the ratio DP/DV is negative, the voltage must be decreased through

$$D((k) = D(k - 1) - \Delta D.$$

The DD crisp value is chosen by trial and tests in simulation. If the crisp value DD is very large or very small, then we may lose information. Despite the fact that the P&O algorithm is easy to implement, it principally has the following problems.

The PV system will always operate in an oscillating mode.

The PV system may fail to track the maximum power point.

3.2 Sliding Mode Controller:

The SMC-MPPT algorithm is divided into two steps. The first is to estimate the actual reference voltage (VMPP) value at which the system will reach its maximum power. The second is the SMC PVG voltage regulation at the VMPP voltage value. These steps lead to a PVG MPP working point. The main role of this controller is to generate a command using a voltage reference (Vref) in order to force the system to work at the maximum power point (MPP). The main novelty in this method is to define the input of the controller as: $V_p = VMPP$. This input can be easily calculated and based on the bijectivity principle between VMPP and PMPP. So if the system will work at the VMPP, the maximum of power will be obtained (PMPP).

Step1: voltage reference estimator

Voltage VMPP value such as, $VMPP = K_v / V_{oc}$, with V_{oc} is the open circuit, or by directly reading and sending VMPP to the regulator [31]. This last requires basically a direct knowledge of the V_{oc} or VMPP values. Generally, users of this method draw the PV characteristics and then feed the target values to the MPPT regulator. This method poorly tracks the VMPP input value that actually changes according to the temperature and depends on the irradiation values as shown in Fig.

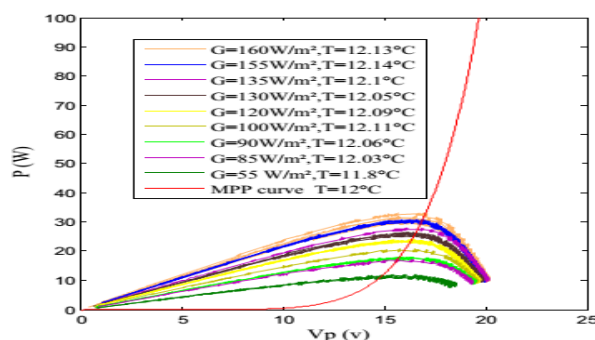


Fig. Real P–V characteristics for different irradiances at almost constant temperature.

Fig. shows that for almost constant temperature and different irradiation values, the maximum power (PMPP) is obtained for different voltage values (VMPP). By joining the different MPP obtained for different irradiation values, we can construct the red curve that for a given (PMPP) value indicates the corresponding VMPP. Therefore, this red curve can be used as a MPP voltage reference estimator constructed using a fitting function F with $VMPP = F(P)$. Fig. explains that for any state, after several iterations (projection), the system will be forced to work with the desired voltage VMPP and hence meets the MPP. For example, assuming that the PV system is working in an operating point 'P1', after projection

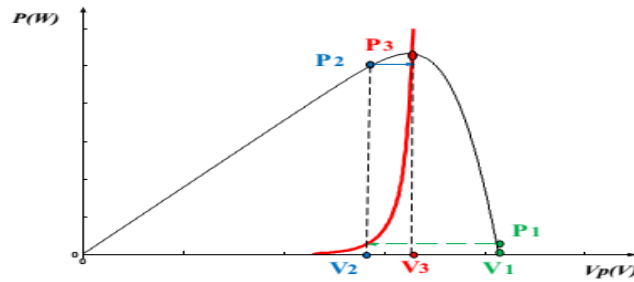


Fig. P–V characteristics at fixed temperature value of 25 C.

Using the reference voltage curve, the reference voltage changes from “V1” to “V2” and consequently the operating point of the PV system will change its position to ‘P2’. Using the same principle, the ‘P2’ will be projected again on the reference curve, and changes its position until the operating point reaches the MPP as shown in Fig. where finally P3 = PMPP. As a result, the constructed red curve can be used as a MPP reference voltage estimator. The main and direct advantage of this approach is that we can overcome the usually required solar radiation sensor.

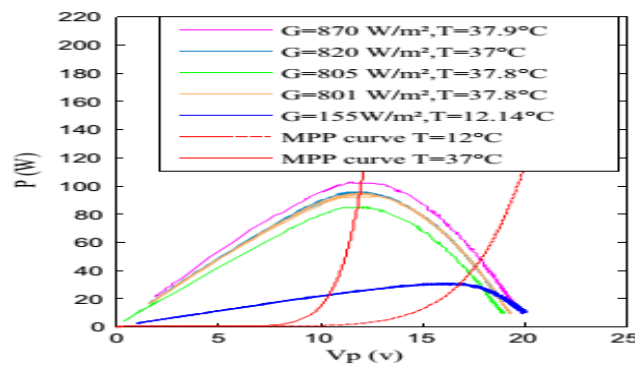


Fig. Real P–V characteristics for different irradiation and temperature values.

Fig. shows the PVG characteristics for different temperature values such as 12 and 37 C. In this figure, the VMPP values are lying between 11.96 V and 16.99 V, which can be considered as a big range. As a result the VMPP is directly connected to the temperature values. As a consequence, one should consider an independent reference voltage curve for each temperature value. In the next part of this paper, the voltage reference (VMPP) estimator is constructed to generate the VMPP for actual temperature values. Since the PV optimal or reference voltage value also depends on the temperature, it is necessary to build an estimator that only considers the temperature values. Fig. 9 presents the curve of the MPP (VMPP = F (PMPP)) power to voltage characteristics for the different couples (VMPP, PMPP) obtained for different conditions. These couples have been collected from real characteristics. All points (VMPP P, T) are interpolated to obtain the function VMPP = F (P, T) which provides the voltage value at the MPP for any power value at a given temperature.

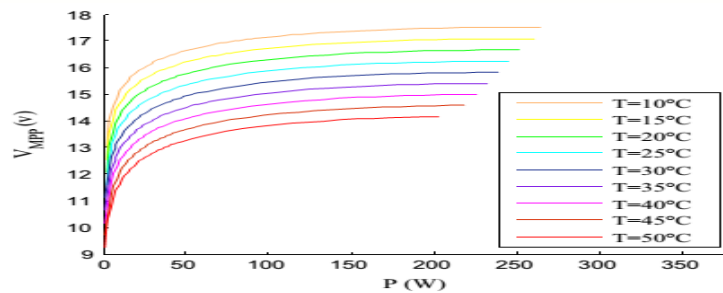


Fig. Optimal power–voltage characteristics for different temperature values.

Several tests have been performed using different types of functions. Finally, it is deduced that the following function provides the better interpolation for the Atersa model. The constructed function is denoted as

$$\begin{aligned}
 V_{MPP} &= F(X, Y) \\
 &= p_{00} + p_{10} * X + p_{01} * Y + p_{20} * X^2 + p_{11} * X * Y + p_{30} * X^3 \\
 &\quad + p_{21} * X^2 * Y + p_{40} * X^4 + p_{31} * X^3 * Y + p_{50} * X^5 \\
 &\quad + p_{41} * X^4 * Y
 \end{aligned} \tag{17}$$

With $X = (P - \text{mean}X) / \text{std}X$ and $Y = (T - \text{mean}Y) / \text{std}Y$
 $\text{mean}X = 73.38, \text{std}X = 67.38; \text{mean}Y = 29.7, \text{std}Y = 13.05$

$p_{00} = 15.29$	$p_{10} = 0.6488$	$p_{01} = -1.09$
$p_{20} = -0.5132$	$p_{11} = 0.01793$	$p_{30} = 0.4582$
$p_{21} = -0.01153$	$p_{40} = -0.2286$	$p_{31} = -0.001497$
$p_{50} = 0.04033$	$p_{41} = 0.001746$	

Fig. shows the surface that provides the reference voltage for different power and temperature values.

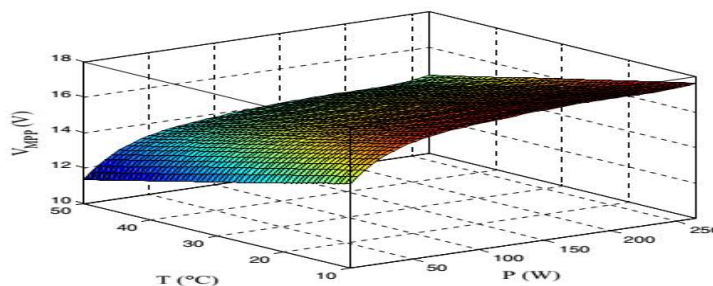


Fig. Surface power–temperature–voltage characteristic of MPP

Step 2: SMC After the estimation of VMPP, the implemented SMC is used to drive the regulation element in such a way to reduce the actual voltage error between the acquired PVG voltage and the target VMPP. The boost converter is forced to bring up the PVG to operate at the desired reference voltage value (Vref) and therefore at the maximum power working point.

$$S = e = V_p - V_{ref} \tag{18}$$

$$u = \frac{1}{2}(1 + \text{Sign}(S)) \tag{19}$$

$$u = \begin{cases} 1 & S > 0 \\ 0 & S < 0 \end{cases} \tag{20}$$

IV. STABILITY DEMONSTRATION

The stability can be analyzed based on the Lyapunov theory. A positive definite function V is defined as:

$$V = \frac{1}{2} S^2 > 0 \tag{21}$$

Whose time derivative is: $\dot{V} = S \frac{dS}{dt} = S \dot{S}$.

$$\text{Considering } \begin{cases} S = e = V_p - V_{MPP}^* \\ \dot{S} = \dot{e} = \dot{V}_p \end{cases}$$

Next, based on the principle of Lyapunov, it is demonstrated that S reaches the state S = 0. Therefore the system reaches the desired voltage value VMPP, and thus reaches the point of maximum power.

When S > 0

The switch will be open; this implies that the duty cycle will increase. From the boost converter model Eq. (16) we have, $R_{pv} = (1 - D)^2 R_{out}$ and using this equation, we can observe that: – If the duty cycle D increases, then R_{pv} decreases, so based on the PV dynamic given by the I–V characteristic shown in Fig, the I_p will increase and V_p will decrease equivalently from Eq. (9). It can be deduced that when the voltage (V_p) increases/decreases, the current (I_p) decreases/increases.

So, as a result in this case, this implies $V_p < 0$ and $S < 0$

Finally, $S \dot{S} < 0$.

When S < 0, Using the same method.

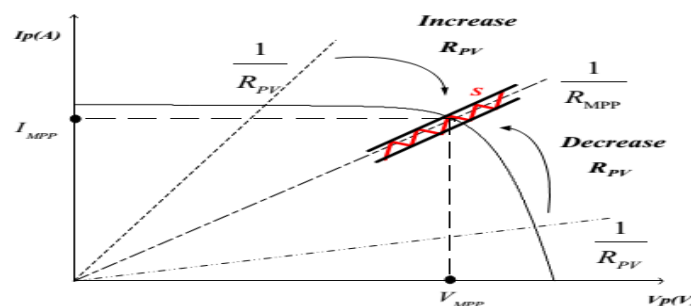


Fig. I–V characteristics and MPPT process.

The switch will be closed this implies that the duty cycle will decrease. If the duty cycle D decreases, then $R_{pv} = (1 - D)^2 R_{out}$ increases. Therefore, based on the PV dynamic given by the I–V characteristic shown in Fig. 11, the I_p will decrease and V_p increases equivalently from Eq. (9). It can be deduced that, when the voltage (V_p) decreases/increases the current (I_p) will increase/decrease, so: If the resistance connected to the PV panel increases then (V_p) increases and (I_p) decreases, this implies that:

$$\dot{V}_p > 0 \text{ and } \dot{S} > 0$$

$$\text{So } \dot{S} < 0$$

Finally, using the Lyapunov stability theory it can be concluded that S reaches the state $S = 0$, meaning that the system reaches the desired voltage value V_{MPP} and hence the converges to the point of maximum power.

V. PARTIAL SHADOWING OF PHOTOVOLTAIC ARRAYS

A number of series/parallel connected PV modules are used to construct a PVG for a desired voltage and current level as previously shown in Fig.3. The performance of the series connected string of the solar cells is unfortunately affected if all its cells are not equally illuminated (partially shaded).

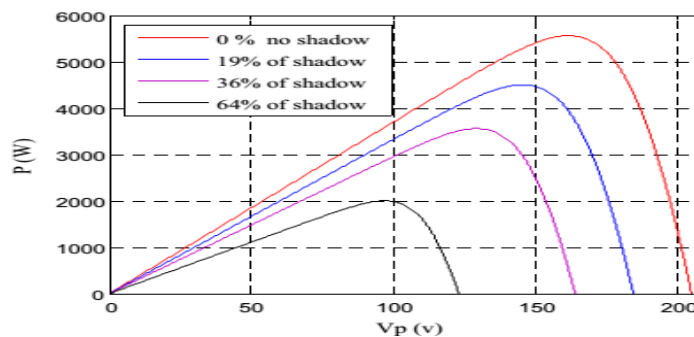


Fig. P–V Characteristics under constant irradiation (1000 W/m²) and temperature (25 C)

Partial shadow (PS) is a common reason of power loss in a photovoltaic application. This loss of efficiency can occurs in many ways. Depending on the object causing the shading, it could only be seasonal, or for a few hours each day, resulting in obviously mysterious fluctuations in the power as shown in Fig. This paper proposes an additional algorithm to be added after the voltage reference estimator and before the SMC controller in order to correctly track the MPP against PS disturbance occurring. This work proposes a system based on a simple partial shadow detection method that will be triggered only when PS is detected; in order to check the presence of a PS, this algorithm makes a test every one second; this is accomplished through the test of the power value. As a result, when the power decreases by 10% the correction action will be triggered. This algorithm is called PS-SMC.

It is divided in three main parts:

Generating the optimal voltage V_{MPP} under ordinary conditions (no partial shadowing), using the voltage reference estimator.

Detection of the partial shadow and search for the new optimal voltage.

Forcing the system to operate with the optimal voltage using the SMC.

In this algorithm, temperature and current voltage sensors are required for the voltage reference estimator. The same current and voltage will be later used for the calculation of the power values. First, the voltage reference

estimator generates the VMMP. After receiving this last value, this algorithm makes a test every period of one second in order to test the existing shadow by detecting a decrease in the power values. In the case of no-existence of power loss, the current VMMP is directly given as an input for the SMC. Otherwise if it detects a decrease of 10% in power quantities (if $DP < 10\%$), the search for the new optimal voltage (new MPP) will begin.

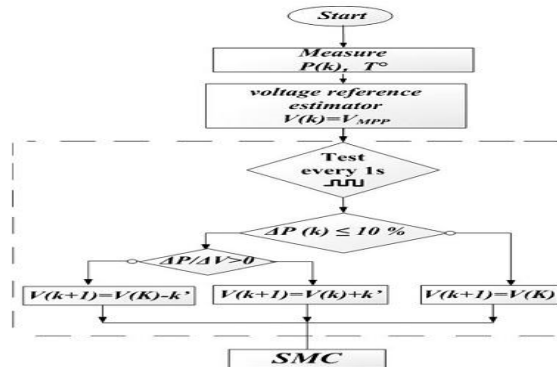


Fig. PS-SMC algorithm flowchart.

This algorithm will start the search from the VMMP to the optimal voltage of the PVG under ordinary conditions. This last voltage is generated by the used voltage reference estimator. In order to minimize the DP/DV ratio value, and starting from the actual VMMP, the voltage is decreased or increased according to the sign of DP/DV with k_0 as a constant of the PS-SMC. Finally, the system operates in the new optimal voltage via the SMC.

VI. RESULTS AND DISCUSSION

The used PV panel contains 10 modules connected in series ($N_s = 10$) and 10 modules connected in parallel ($N_p = 10$) as shown in Fig. The PS-SMC, with optimal voltage reference, is compared to P&O algorithm. Both controllers are tested over external and internal variation. The system is tested over a sudden step irradiation and load changes as shown respectively in Fig's. This action is used to prove the controller robustness and the ability to keep extracting the maximum power within this abrupt variation. In order to test the PS-SMC robustness against PS the system will suffer 19% of partial shadowing from 1 to 3 s as shown in Fig.

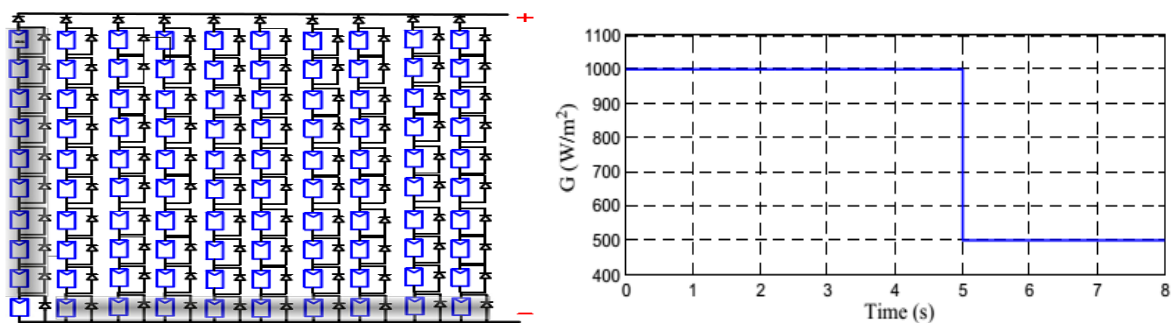


Fig. PV array configuration.

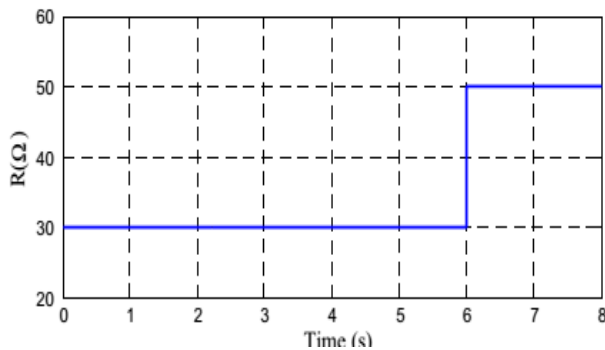


Fig. Irradiation abrupt variation.

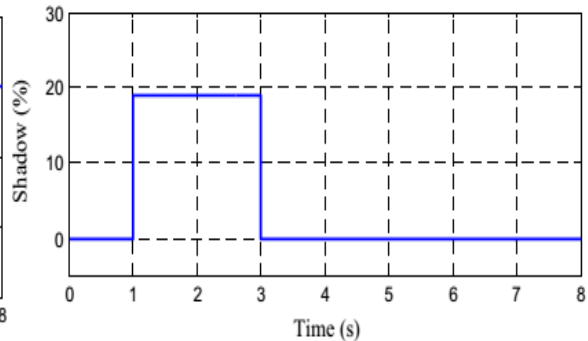


Fig. Load abrupt variation.

Fig. Partial shadow abrupt variation.

The results shown in Fig's demonstrate the obtained results of P&O and the PS-SMC tracker's stability. The PS-SMC has very short response time and overshoots. Moreover, PS-SMC presents a reduced oscillation signal in the MPP compared with the P&O one. Below Fig. presents the duty cycle signal delivered by the P&O algorithm, which will be used with a reference saw signal to generate a PWM IGBT drive signal. Fig. also shows the direct PWM signal generated by the PS-SMC.

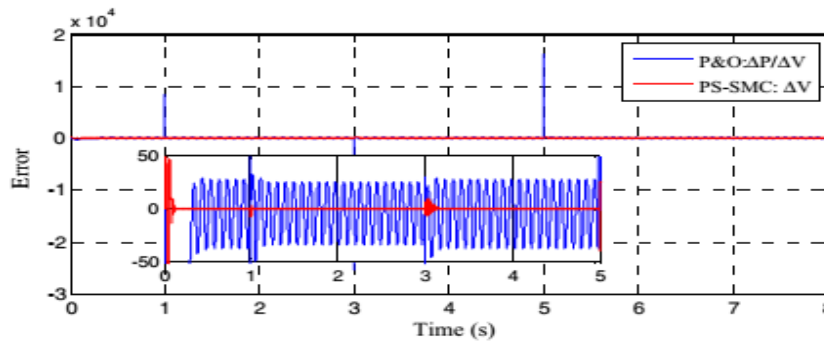


Fig. Controllers Performances.

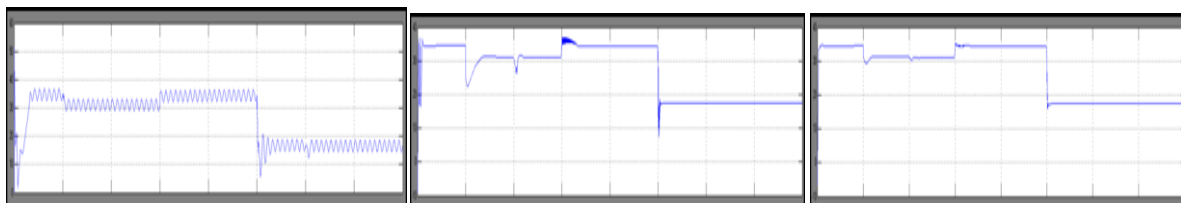


Fig : PVG current behavior (a) using P&O (b) using SMC (c) using FUZZY

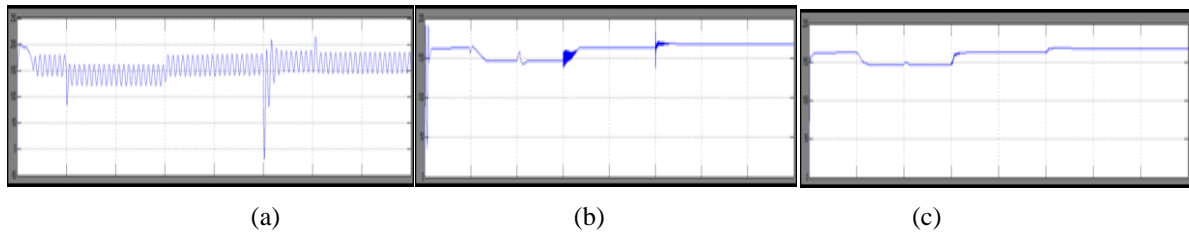


Fig : PVG voltage behavior (a) using P&O (b) using SMC (c) using FUZZY

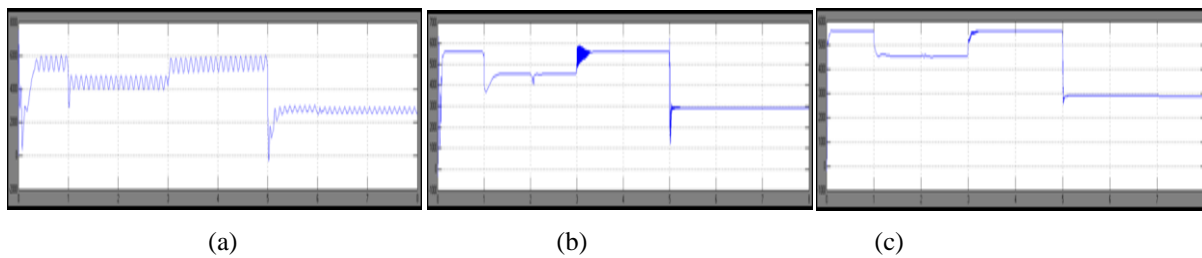


Fig : PVG power (a) using P&O (b) using SMC (c) using FUZZY

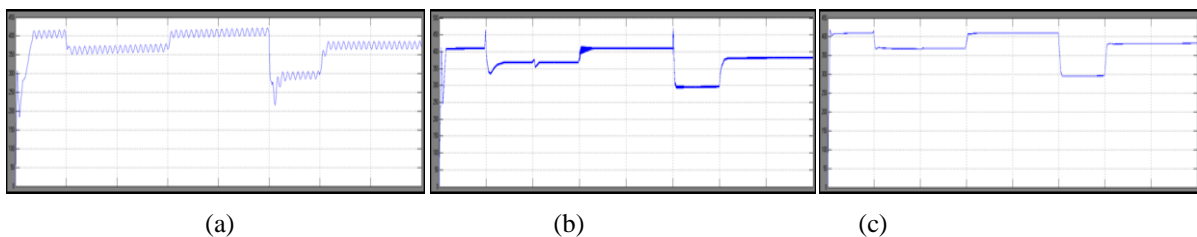


Fig : The load feeding voltage (a) using P&O (b) using SMC (c) using FUZZY

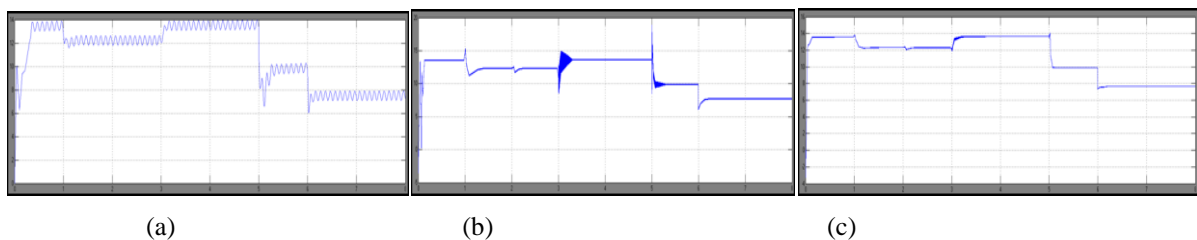


Fig : The load current (a) using P&O (b) using SMC (c) using FUZZY

VII. CONCLUSION

A PVG system feeding a passive load type through a Boost converter is studied through simulation tests and practical implementation. To improve the system efficiency and performance, a MPPT DC–DC converter driven is synthesized based on the sliding mode theory. The stability of the proposed SMC-MPPT system is verified using the Lyapunov theory. To perform an accurate and rapid SMC-MPP tracker, a simple and reliable estimator was constructed using only temperature and power sensors. This estimator generates the VMPP according to

simultaneous temperature and irradiation variations. It is dressed in an analytical form to be easy to implement. The proposed MPPT algorithm ensures robustness and high tracking performance. To compensate and overcome the PVG shadowing effects and drawbacks, a new algorithm is proposed PS-SMC. Many tests were performed in an extensive simulation work to verify the robustness and the high performance of the proposed PS-SMC algorithm against partial shadow, load profile, and irradiation variations. Obtained results were presented and discussed. A practical implementation work was performed yielding a real prototype for implementation of the used algorithm. Experimental results and practical setup are described and discussed for the PVG system with a SMC-MPPT. This paper summarizes the main algorithms driving an entire PVG system obtained after long and extensive work, which dealt with theoretical and experimental efforts. Acquired results are very encouraging and suggest perspective experimental and theoretical studies for boosting PVG system performances. Moreover, this work can be extended to consider dynamic load types.

REFERENCES

- [1] Farhat M, Flah A, Sbita L. Photovoltaic maximum power point tracking based on ANN control. *Int Rev on Model Simul (IREMOS)* 2014;7:474–80.
- [2] Zakzouk NE, Abdelsalam AKA, Helal A, Williams BW. Modified variable-step incremental conductance maximum power point tracking technique for photovoltaic systems. In: 39th Annual conference of the IEEE industrial electronics society. *IECON*; 2013. p. 1741–8.
- [3] Hadji S, Gaubert J, Krim F. Maximum Power Point Tracking (MPPT) for photovoltaic systems using open circuit voltage and short circuit current. In: *IntConfSyst Control (ICSC)*. p. 87–92.
- [4] El Khateb A, Rahim NA, Slvarj J, Uddin MN. Fuzzy logic controller based SEPIC converter for maximum power point tracking. *IEEE Trans Ind. Appl.* 2014;50:2349–58.
- [5] Farhat M, Barambones O, Sbita L. Efficiency optimization of a DSP-based standalone PV system using a stable single input fuzzy logic controller. *Renew Sustain Energy Rev* 2015;49:907–20.
- [6] Alqahtani A, Utkinin V. Self-optimization of photovoltaic system power generation based on sliding mode control. In: *Proceedings of IECON'12*. p. 3468–74.
- [7] Levron Y, Shmilovitz D. Maximum power point tracking employing sliding mode control. *IEEE Trans Circuits Syst* 2013;60:724–31. [8] Cid-Pastor A. Synthesis of loss-free resistors based on sliding-mode control and its applications in power processing. *Control EngPract* 2013;21:689–99.
- [9] Oscar LL, Maria TP, Manel GA. New MPPT method for low-power solar energy harvesting. *IEEE Trans Industr Electron* 2010;57:3129–38.
- [10] Elgendy M, Zahawi AB, Atkinson DJ. Comparison of directly connected and constant voltage controlled photovoltaic pumping systems. *IEEE Trans Sustain Energy* 2010;1:184–92.
- [11] Xianwen G, Shaowu L, Rongfen G. Maximum power point tracking control strategies with variable weather parameters for photovoltaic generation systems. *Sol Energy* 2013;93:357–67.
- [12] Jubaer A, Zainal S. An improved perturb and observe (P&O) maximum power point tracking (MPPT) algorithm for higher efficiency. *Appl Energy* 2015;150:97–108.

- [13] Saravanan S, Ramesh Babu N. Maximum power point tracking algorithms for photovoltaic system – a review. *Renew Sustain Energy Rev* 2016;5:192–204.
- [14] Mohammadi A, Mezzai N, Rekioua D, Rekioua T. Impact of shadow on the performances of a domestic photovoltaic pumping system incorporating an MPPT control: a case study in Bejaia, North Algeria. *Energy Convers Manage* 2014;84:20–9.
- [15] Alsayid AB, Alsadi SY, Jallad JS, Dradi MH. Partial shading of PV system simulation with experimental results. *Smart Grid Renewable Energy* 2013;4:429–35.
- [16] Sun Y, Chen S, Xie L, Hong R, Shen H. Investigating the impact of shading effect on the characteristics of a large-scale grid-connected PV power plant in Northwest China. *Int J Photoenergy* 2014. <http://dx.doi.org/10.1155/2014/763106>. 9 pages 763106.
- [17] Gao L, Dougal RA, Liu S, Iotova AP. Parallel-connected solar PV system to address, partial and rapidly fluctuating shadow conditions. *IEEE Trans Indust Electron* 2009;56:1548–56.
- [18] Anusuya C, Venkatasubramanian S. Design and implementation of solar power optimizer for DC distribution system using dual active bridge. *Int J Adv Res Elect Electron Instrument Eng* 2014;3:168–73.
- [19] Muthuramalingam M, Manoharan PS. Comparative analysis of distributed MPPT controllers for partially shaded stand alone photovoltaic systems. *Energy Convers Manage* 2014;86:286–99.
- [20] Rizzo S, Scelba G. ANN based MPPT method for rapidly variable shading conditions. *Appl Energy* 2015;145:124–32.
- [21] Farhat M, Sbita L. Efficiency boosting for PV systems-MPPT intelligent control based. *Energy Efficiency*. Intech Publisher; 2015. <http://dx.doi.org/10.5772/59399>.
- [22] Farhat M, Fleh A, Sbita L. Influence of photovoltaic DC bus voltage on the high speed PMSM drive. In: 38th Annual conference of the IEEE industrial electronics society 2012, 25–28 October, Montreal, Quebec, Canada.
- [23] Muthuramalingam M, Manoharan PS. A photovoltaic power system using a high step-up converter for DC load applications. *Energy Convers Manage* 2014;86:286–99.
- [24] Zhou Z, Holland PM, Iqic P. MPPT algorithm test on a photovoltaic emulating system constructed by a DC power supply and an indoor solar panel. *Energy Convers Manage* 2014;85:460–9.
- [25] Fernão PV, Romero-Cadaval E, Vinnikov D, Roasto I, Martins JF. Power converter interfaces for electrochemical energy storage systems – a review. *Energy Convers Manage* 2014;86:453–75.
- [26] Shameem A, FadiMAI, Saad M, Hazlie M. Fuzzy based controller for dynamic Unified Power Flow Controller to enhance power transfer capability. *Energy Convers Manage* 2014;79:652–65.
- [27] Guerrero-Rodríguez NF, Alexis BB. Modelling, simulation and experimental verification for renewable agents connected to a distorted utility grid using a Real-Time Digital Simulation Platform. *Energy Convers Manage* 2014;84:108–21.
- [28] Her TY, Chih JL, Qin CL. PSO based PI controller design for a solar charger system. *Sci World J* 2013;1–13.
- [29] Farhat M, Barambones O, Sbita L, Fleh A. A robust MPP tracker based on sliding mode control for a photovoltaic pumping system. *Int J Automat Comput*, in press.

- [30] Rújula AAB, Abián JAC. A novel MPPT method for PV systems with irradiance measurement. *Sol Energy* 2014;109:95–104.
- [31] Liu C, Wu B, Cheung R. Advanced algorithm for MPPT control of photovoltaic system. In: *Canadian Solar Buildings Conference Montreal*, August 20–24, 2004.
- [32] Abderrahim EF, Fouad G, Abdelmoinime M. Reference voltage optimizer for maximum power tracking in single-phase grid-connected photovoltaic systems. *J Control SystEng* 2013;12:57–66.
- [33] Farhat M, Barambones O, Ramos JA, Durana JMG. Maximum power point tracking controller based on sliding mode approach. In: *Actas de las XXXV Jornadas de Automática, Valencia*, 3–5 de septiembre, 2014.
- [34] MathurBadrilal. Effect of shading on series and parallel connected solar PV modules. *Modern ApplSci* 2009;3:32–41.
- [35] Benyoucef As, Chouder A, Kara K, Silvestre S, Sahed OA. Artificial bee colony based algorithm for maximum power point tracking (MPPT) for PV systems operating under partial shaded conditions. *Appl Soft Comput* 2015;32:38–48.
- [36] Farhat M, Sbita L. ANFIS controlled solar pumping system. *i-Manager's J Electron Eng* 2011;2:1–9.
- [37] Farhat M, Barambones O, Fleh A, sbita L. Variable structure MPP controller for photovoltaic pumping system. *Trans Inst Measure Control* 2016:1–10.
- [38] Rezk H, Eltamaly AM. A comprehensive comparison of different MPPT techniques for photovoltaic systems. *Sol Energy* 2015;112(February):1–11.
- [39] Esram T, Chapman P. Comparison of photovoltaic maximum power point tracking techniques. *IEEE Trans Energy Convers* 2007;22:439–49.
- [40] Fröhlich AA, Bezerra EA, Slongo LK. Experimental analysis of solar energy harvesting circuits efficiency for low power applications. *ComputElectrEng* 2015;45:143–54.
- [41] Valencia PAO, Paja CAR. Sliding-mode controller for maximum power point tracking in grid-connected photovoltaic systems. *Energies* 2015;8:12363–87.
<http://dx.doi.org/10.3390/en81112318>.